SHORELINE CHANGE PROJECTION CONSIDERING THE UNCERTAINTY CAUSED BY MULTIPLE FACTORS UNDER CLIMATE CHANGE

Kunihiro Watanabe[1], Fuminori Kato[2], Akiyoshi Katano[3] and Yoji Tanaka[4]

Climate change adaptation represents a critical challenge in contemporary beach management. While the majority of previous researches has concentrated on erosion caused by sea level rise, the effects of future change in wave conditions and storm surges have not been sufficiently explored. To address this, we have developed a new method for projecting shoreline changes, which allows for the simultaneous calculation of changes induced by sea level rise and longshore sand transport. Subsequently, we have conducted parametric studies to assess the influence of multiple variables on future shoreline changes, and demonstrated the importance of accurate estimation of sediment supply from rivers.

Keywords: climate change; shoreline change; numerical simulation; uncertainty

INTRODUCTION

The rise in sea level poses a significant challenge for beach management as a consequence of climate change. Numerous studies have employed the Bruun rule to simulate future shoreline changes (e.g. Udo and Takeda 2017). The Bruun rule is the most widely adopted method for predicting shoreline response to sea level rise (SLR). Nevertheless, it has faced considerable criticism regarding the validity of its assumptions (e.g. Copper and Pilkey 2004). While the Bruun rule is effective for identifying general trends over extensive areas, it lacks the precision required for formulating adaptation measures to counter coastal erosion induced by the SLR.

One notable shortcoming of the Bruun rule is the assumption that the total sediment volume is conserved within the cross-section. Under this premise, the active portion of an offshore profile rises with the rising sea level, and the sand required to elevate the profile is transported from the shoreline. Figure 1 illustrates a schematic of the profile changes, depicting a translation of the beach profile by a shoreline change ΔX following a rise ΔS in sea level, resulting in shoreline retreat and sediment deposition. This concept is fundamentally two-dimensional and is not applicable to three-dimensional assessments. Furthermore, the Bruun rule primarily address erosion rather than accretion. These limitations were also acknowledged by Bruun, who proposed boundary conditions and adjustments to make the rule more practical and realisitc (Bruun 1983).

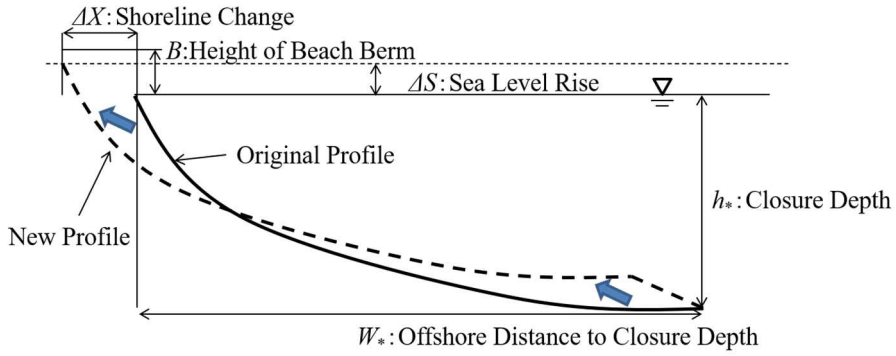

Figure 1. Active profile changes due to sea level rise according to the Bruun rule.

Dean and Houston (2016) introduced an equation that emcompasses all phenomena impacting on shoreline change, including Bruun rule recession, onshore transport, sand sources and sinks, and longshore transport gradients. This method is applicable to open beaches where the sediment volume within cross-section varies over time due to longshore sediment tramsport. However, Dean and Houston (2016)'s method has two primary shortcomings: the determintion of equilibrium profile and the additional computational cost. The Bruun rule recession is calculated based on the assumption that active

[1] Kochi Office of River and National Highway, Ministry of Land, Infrastructure, Transport and Tourism Shikoku Regional Development Bureau, 96-7 Rokusenji-cho, Kochi City, Kochi, 780-0026, Japan.
[2] National Institute for Land and Infrastructure Management, 1 Asahi, Tsukuba City, Ibaraki, 305-0804, Japan.
[3] Ecoh Corporation, 2-6-4 Kita-Ueno, Taito-Ku, Tokyo, 110-0014, Japan.
[4] Ecoh Corporation, 2-6-4 Kita-Ueno, Taito-Ku, Tokyo, 110-0014, Japan.

portion of a profile maintains a constant form, known as an equilibrium profile (Dean and Houston 2016). This equilibrium profile depends primarily on sand size and wave parameters. Dean (2002) proposed a simple equation using the A parameter for the area above an equilibrium profile of the form $h = Ay^{2/3}$ out to a distance y and a depth h. Although most studies have utilized this relationship, the A parameter recomended by Dean (2002) is limited to sediment size below 1.09 mm. Dean's equilibrium profile should be translated into a physics-based model to enable the projection of future shoreline changes on various types of local beaches.

When considering the computational cost, Dean and Houston (2016)'s equation includes an additional term representing the longshore transport gradients. This arrangement allows for the consideration of shoreline changes induced by lognshore sediment transport. The term for the longshore transport gradient can be relatively easily applied to coasts with simple seabed topography and no artificial structures. However, for coasts with complex seabed topography or numerous artificial structures, wave transformation calculations are required. This additional procedure negate the advantage of the Bruun rule, which allows for easy estimation of future shoreline changes.

While most attention has been focused on erosion induced by SLR, it is essential to project other coastal drivers, including waves and storm surges. Therefore, methods that incorporate projections of climate change related drivers beyond SLR and employ physics-based models to simulate shoreline changes due to various forcing mechanisms are necessary (Toimil et al. 2020). Future changes in wave characteristics are crucial for predicting shoreline changes, as future changes in wave direction can significantly influence the direction of nearshore sand transport. For instance, Shimura and Mori (2019) projected future wave climate using results of a global climate model, demonstrating that the mean wave direction would shift counterclockwise on the Japan Sea side and clockwise on the Pacific side of east Japan. Additionally, sediment balance and land subsidence must be considered when projecting shoreline changes on eroded coasts. Although Dean and Houston (2016) revised the Bruun rule to consider the longshore sediment transport, they did not investigated the changes in longshore sediment transport caused by future wave climate change.

Ranasinghe et al. (2016) identified the potential primary impacts of climate change on open sandy coasts, selecting mean sea level, wave conditions, storm surges, and river flow as the four key environmental drivers. Başaran and Arı Güner (2024) explored the future wave climate-driven longshore sediment transport and shoreline change under the RCP4.5 and RCP8.5 wave climate scenarios. They calculated shoreline changes over a specified period by considering temporally and spatially varying longshore sediment transport. However, Başaran and Arı Güner (2024) employed a model based on the one-line theory for shoreline change modeling. Their model assumes that the cross-shore profile remains unchanged during erosion and accretion, and they made slight adjustments to obtain accurate results.

The Bruun rule provide a single deterministic estimate of future coastline change. This may be inadequate for coastal planning based on the SLR assumption, which holds uncertainty. Ranasinghe et al. (2012) proposed a probabilistic coastline recession (PCR) model to obtain probabilistic estimates of SLR-driven coastline recession. The physical processes governing coastal recession due to SLR are explicitly taken into account, and estimates of coastal recession are provided within a probabilistic framework in the PCR model. The PCR model considers probability by generating time series of storms using data derived from joint probability distributions of storm characteristics within a Monte Carlo simulation. However, applicability of the PCR model has not been sufficiently evaluated, as Ranasinghe (2012) investigated the model on a survey profile where the potential impact of longshore sediment transport is minimal.

Although Ranasinghe (2012) accounted for the uncertaintity induced by variations of storm characterisitics, other factors could contribute to the uncertaintity in the future shoreline change projections. Once we determine the impact of each factor on overall uncertainty, we need to focus on the most influential factors for future shoreline change projectons.

Based on the studies reviewed, three areas for improvement have been identified. First, we need to represent SLR-induced changes in cross-sectional topography using a physics-based model. This will expand applicability of shoreline projections to a wide range of sandy beach conditions. Second, it is essential to consider factors other than SLR. Finally, it is necessary to identify the factors that have the most significant impact on the overall uncertainty of future shoreline changes. In this study, we propose a new projection method that takes into account changes in wave characteristics and other factors, and conducted parametric studies to evaluate the influence of multiple factors on future shoreline changes.

MATERIALS AND METHODS

Beach deformation Models

We modified a typical contour line change model based on Serizawa et al. (2003) to calculate shoreline change induced by SLR and longshore sand transport simultaneously. In this model, cross-shore sediment transport is determined by the balance between the equilibrium slope of sand β_c and local slope β (Eq. 1, Eq. 2, and Eq. 3). The shoreline changes, which are assumed to occur to maintain the equilibrium beach profile under sea level rise as described by the Bruun rule, are expected to be represented by this arrangement. These shoreline changes due to cross-shore sand transport are not a short-term beach change associated with storm waves, but a long-term beach changes with a time scale comparable to that of beach changes due to longshore sand transport.

$$h_k \frac{\partial y_k}{\partial t} + \left[\frac{\partial Q_k}{\partial x} + \frac{\partial q_z}{\partial z}\right] = 0 \tag{1}$$

$$q_z = \varepsilon_z(z) \cdot K_z \cdot \left(EC_g\right)_b \cdot \sin\beta_c \cdot \left(\frac{\cot\beta}{\cot\beta_c} - 1\right) \tag{2}$$

$$\int_{-h_c}^{h_R} \varepsilon_z(z)dz = 1 \tag{3}$$

where h_k: vertical interval of contour line k, y_k: horizontal distance of contour line k, Q_k: the amount of longshore sediment transport in contour line k, $\varepsilon_z(z)$: distribution of cross-shore sediment transport, k_z: coefficient of cross-shore sediment transport, $\left(EC_g\right)_b$: wave energy flux at the breaking point, h_R: upper limit height of sediment transport, h_c: closure depth of sediment transport.

The amount of longshore sediment transport along contour line k represented as Q_k was calculated by multiplying Q by cofficient μ_k (Eq. 4). The cofficient μ_k signifies the ratio of longshore sediment transport along contour line k to the total sediment transport (Eq. 5). Eq. 6 represents the Ozasa and Brampton sediment transport term (Ozasa and Brampton, 1980). The depth distribution of longshore sediment transport was calculated based on the rerationship proposed by Uda and Kawano (1996) (Eq. 7).

$$Q_k = \mu_k \cdot Q \tag{4}$$

$$\mu_k = \int_{Z_k}^{Z_{k+1}} \xi(z)\,dz \Big/ \int_{-h_c}^{h_R} \xi(z)\,dz \tag{5}$$

$$Q = \frac{\left(EC_g\right)_b}{(\rho_s - \rho)g(1-\gamma)}\left(K_1 \sin\alpha_b \cos\alpha_b - K_2 \cos\alpha_b \cot\beta \frac{\partial H_b}{\partial y}\right) \tag{6}$$

$$\xi(z) = \begin{cases} = \dfrac{2}{h_c^3}\left(\dfrac{h_c}{2} - z\right)(z + h_c)^2 & (-h_c \le z \le h_R) \\ = 0 & (z < -h_c, h_R < z) \end{cases} \tag{7}$$

where Z_k and Z_{k+1}: lower and upper boundary depth of contour line k, ρ: density of water, ρ_s: density of sediment, g: glavity acceleration, γ: porosity of sediment, K_1: cofficient of longshore sediment transport, K_2: longshore sediment transport cofficient relative to wave steepness, α_b: wave breaking angle against shoreline, H_b; wave breaking height.

The aforementioned model assumes uniform grain size. To account for beaches composed of mixtures of different sand sizes, the contour change model was expanded following the methodologies of Tanaka and Suzuki (1998) and Kumada et al. (2002). In this expanded model, sediment sizes were divided into N categories, introducing $K = 1, 2, \ldots, N$. The cofficient of longshore sediment transport K_1 was modified to $K_1(K)$ to consider the relationship between the coefficient $K_1(K)$ and grain size $D(K)$, as outlined by Kamphius et al. (1986). The amount of longshore sediment transport along contour line k for each grain size was represented as $Q_k(K)$, and calculated by Eq. 8, Eq. 9 and Eq. 10.

$$Q_k(K) = \varepsilon_k \cdot \mu_k(K) \cdot K_1(K) \cdot F_x \tag{8}$$

$$F_x = \frac{(EC_g)_b}{(\rho_s - \rho)g(1-\gamma)}\left(\sin\alpha_b \cos\alpha_b - K_2' \cos\alpha_b \cot\beta \frac{\partial H_b}{\partial y}\right) \tag{9}$$

$$K_1(K) = A\big(D(K)\big)^{-1/2} \tag{10}$$

where ε_k: cofficient for longshore sediment transport on contour line k, $\mu_k(K)$: content ratio of grain size Kon contour line k, K_2' : longshore sediment transport cofficient relative to wave steepness.

The coefficients of sediment transport were calibrated using hindcast calculations of past shoreline changes at the study site, explainded later, between 1969 and 2019.

Study Site

Future shoreline changes were projected for the Suruga coast (Shizuoka Prefecture), located in the central Japan and facing the Pacific Ocean (Fig. 2, and Fig.3). The bathymetry of Suruga Coast is steep, and an underwater valley is situated close to the shore at the northern end of the coast. Approximately 30,000 m^3/year of sediment is discharged into this underwater valley. Oi River flows into Suruga Coast, supplying about 280,000 m^3/year of sediment to both sides of the river mouth. However, the northward movement of sediment obstructed by a breakwater at Oigawa Port. Suruga Coast has experienced erosion due to a decrease in sediment supply from the Oi River and the obstruction of longshore sediment movement by Oigawa Port (Fig. 4). To mitigate this coastal erosion, the construction of detached breakwaters and beach nourishment has been implemented since 1964. Crustal movement induced by plate tectonics has caused land subsidence around the Suruga Coast. For instance, the ground near Cape Omaezaki has subsided by 4cm over the past 10 years, and similarly, the ground near the Suruga Coast has sunk 3cm over the same period.

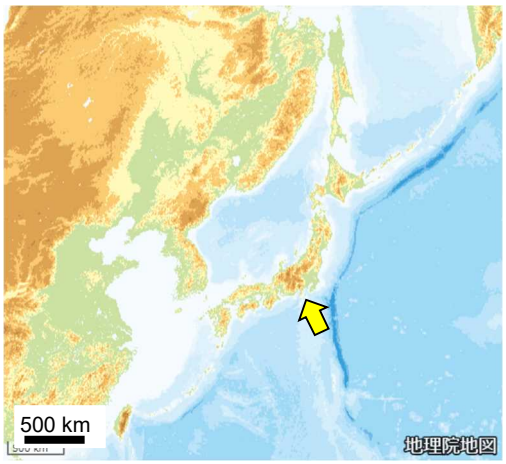

GSI MAP (https://maps.gsi.go.jp/)

Figure 2. Location of Suruga Coast around Japan.

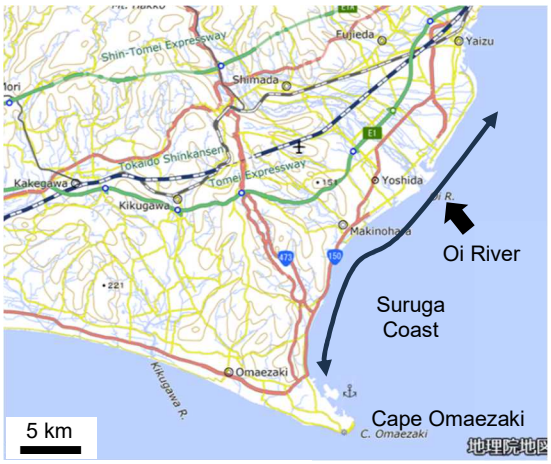

GSI MAP (https://maps.gsi.go.jp/)

Figure 3. The location of Cape Omaezaki and Oi River on the Suruga Coast.

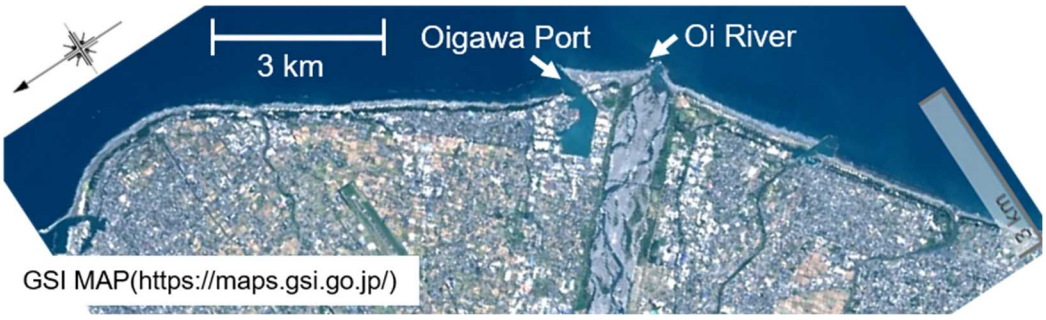

Figure 4. Aerial image of Suruga coast.

Coastal Sediments on the Suruga Coast

The coastal sediments were assumed to be composed of mixed-sized sediments. The main beach sediments are gravel at depths shallower than 2-7 m, and sand at greater depths. The total contour line change at a specific position was determined by summing the contour line changes of all grain size populations (Kumada et al. 2007). Nine categories of grain size populations were assumed, and the equilibrium slopes $\tan\beta_c$ were defined as 1/140, 1/85, 1/15, for grain size 0.05-0.1 mm, 0.1-0.4 mm, 0.4-1.0 mm, and 1/6 for coarser grains.

Uncertainty in Multiple Factors

We estimated the potential range of shoreline changes using 252 projections based on combinations of sea level and wave conditions, ground subsidence due to tectonics, sediment supply from the river, and sediment discharge to undersea valley over 100 years (Table 1, Table 2, Table 3 and Table 4). The degree of change in sea level and wave conditions was assumed based on projections around Japan (MEXT and JMA 2020, Shimura and Mori 2019). Future sea level was assumed to rise linearly and changed every 10 years. Three types of conditions-the avarege, 95 % upper limit, and 95 % lower limit of sea levels-were applied for each Representative Concentration Pathways senario (RCP2.6 and RCP8.5). We conducted calculations under these six conditions (W2 - W7), in addition to the current condition (W1) that does not consider climate change, making a total of seven conditions (Table 1).

The current wave conditions were set using wave observation data obtained off the Cape Omaezaki. Future wave conditions were assumed based on the future wave climate projections conducted by Shimura and Mori (2019). Bias corrections were applied on the wave frequency spectrum of these projections using the method proposed by Watanabe et al. (2024), and the avareged height and period of waves were calculated in three major directions. In shoreline change simulations, the wave conditions were updated monthly to coincide with the ratios in three wave directions (Table 2). The average wave height and period in all directions in RCP 2.6 are greater than the current conditions, and the average wave directions in RCP 2.6 shifts 3.2 degrees clockwise from the current direction (Table 3). Conversely, the average wave height in RCP 8.5 is smaller than the current status, and the average wave direction in RCP 8.5 shifts 6.8 counterclockwise from the current direction.

The average, upper limit, and lower limit of other factors, such as ground subsidence (C1 - C4), sediment supply (R1 - R3), and sediment discharge to the undersea valley (S1 - S3), were determined based on the published literature (Table 4). Future performance changes of detached breakwaters were previously investigated using a numerical wave flume called CADMAS-SURF (e.g. Isobe et al. 1999) and applied to wave deformation calculations.

Table 1. Conditions of sea level and wave.

Case	Sea level	Wave condition
W1	Current status	Current status
W2	RCP 2.6 95% upper limt	RCP 2.6
W3	RCP 2.6 average	RCP 2.6
W4	RCP 2.6 95% lower limt	RCP 2.6
W5	RCP 8.5 95% upper limt	RCP 8.5
W6	RCP 8.5 average	RCP 8.5
W7	RCP 8.5 95 lower limt	RCP 8.5

Table 2. Height, period, direction of waves on each scenario.

	Ratio (%)	Height (m)	Period (s)	Direction (degree)
Current Status	28.38	1.05	6.21	97.5
	24.74	1.36	6.90	135.6
	46.88	1.07	6.31	168.7
RCP 2.6	28.38	1.07	6.57	100.7
	24.74	1.39	7.30	138.8
	46.88	1.09	6.68	171.9
RCP 8.5	28.38	0.99	6.34	90.7
	24.74	1.28	7.04	128.8
	46.88	1.01	6.44	161.9

Table 3. The annual average wave height, period and direction.

	Height (m)	Period (sec)	Direction (degree)
Current Status	1.15	6.43	140.0
RCP 2.6	1.17	6.80	143.2
RCP 8.5	1.09	6.56	132.2

Table 4. Conditions of ground subsidence by tectonics, sediment supply from the river and sediment discharge to undersea valley.

Ground subsidence by tectonics		Sediment supply from the river		Sediment discharge to undersea valley	
Case	mm/y	Case	$\times 10^4$ m^3/y	Case	$\times 10^4$ m^3/y
C1	3.7	R1	27.9	S1	3.0
C2	3.7 with an uplift in the 30th year	R2	169.0	S2	1.0
C3	3.7 with an uplift in the first year	R3	32.2	S3	4.7
C4	No subsidence				

RESULTS

Validation of the Simulation Model

The applicability of this simulation model to SLR was investigated by calculating the contour line change on a model beach composed of a single grain size with simple topography. The wave height and period were assumed to be the mean energy waves, set at 1.4 meters and 8.0 seconds, respectively. The sediment size was assumed to 1.0 mm, and 1.0 was applied as the coefficient of cross-shore sediment transport (k_z).

The simulation results were consistent with the shoreline retreat estimated using the Bruun rule (Fig. 5). The beach profile retreated at elevations ranging from 0 m to 3 m, maintaing its cross-sectional shape at these elevations. The holizontal shoreline position in the model retreated 69 meters from the initial position, while the shoreline retreat calculated based on the Bruun rule was 91 meters. The offshore topography naturally converged on a closure depth of 8 meters.

Future Projections

The results of the future projections showed significant variations in shoreline changes along the coast. The shoreline advanced offshore around the mouth of the Oi River (x= 9,000-10,000 m) and Oigawa port (x = 8,000 m), with greater variations in shoreline change observed around the river mouth (Fig. 6). The shoreline retreated in the section west of Oigawa port (X = 0-7,000 m), with the degree of shoreline retreat varying in front of the undersea valley (x= 1,000-2,000 m). On the coast east of Yoshida Fishing Port (x= 12,500-15,000 m), the direction of shoreline change varied depending on the calculation conditions; however, it generally tended to retreat.

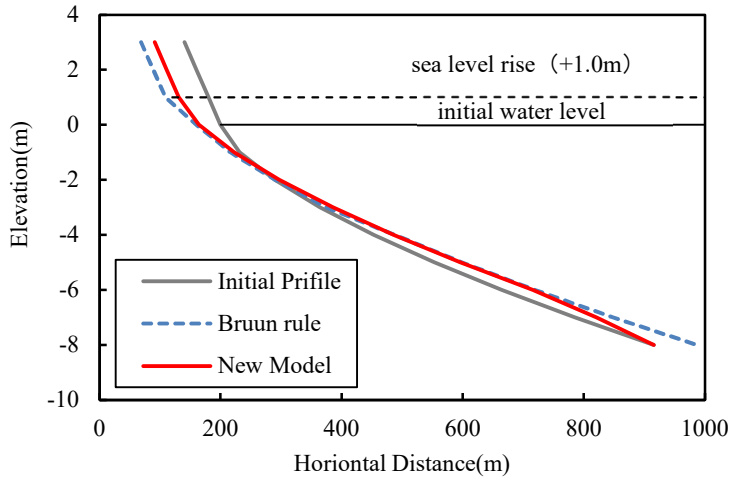

Figure 5. Change in beach profile calculated under sea level rise.

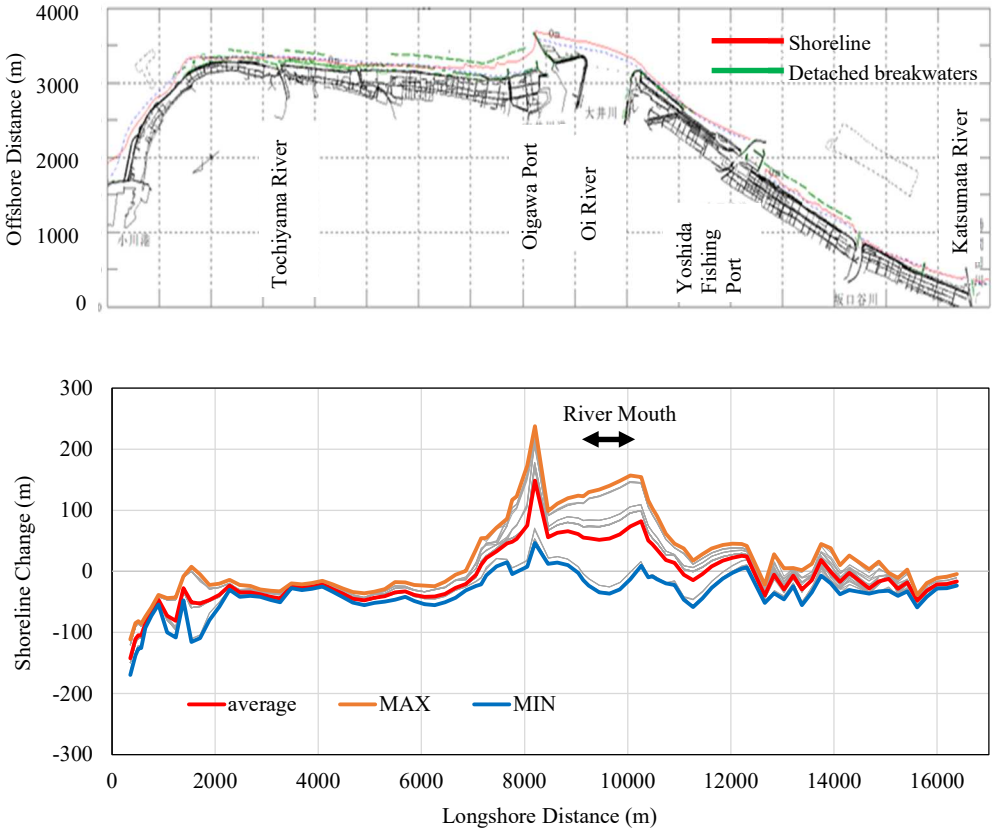

Figure 6. Distribution of coastal facilities along the Suruga coast (above), and shoreline changes (below) calculated under the assumption of sea level rise and wave condition based on IPCC AR5-RCP scenario 8.5 average (W6 in Table 1.)

Shoreline Change Variation

The contribution of each factor to shoreline change variation was evaluated using 10 representative survey lines. Shoreline changes exhibited significant deviations, particularly near the river mouth. The sand supply from the river emerged as the most influential factor for the deviations, especially in the survey lines located at a longshore distance of 6,000-12,000 meters.

Figure 7 illustrates the variarions in caluculated shoreline changes among cases extracted under the same condition in survey line #36 (longshore distance x = 6,260 m). This survey line was selected because it is located on the downdrift of the alongshore drift from Oigawa port and is considered to be a representative transect of this coastline's typical features.

The box plot for case R1 was derived from the calculation results of 84 cases, which were calculated under the condition assuming 279,000 m^3/year of sediment supply from the river. Box plots for cases R2 and R3 were derived from the calculation assming lower and higher sediment supply than case R1, respectively (Table 4). Shoreline changes ranged from -48.7 meters (upper quatile) to -65.2 meters (lower quatile) for case R2, and from -11.1 meters (upper quatile) to -30.0 meters (lower quatile) for case R3 (Fig. 7). The variations in the calculation results due to differences in sediment supply from river were greater than the range of results for each condition. These results clearly indicate that differences in sediment supply lead to significant differences in future shoreline changes.

Box plots of shoreline changes with different timing of ground subsidence due to tectonics (Cases C1-C3) did not show any diffrence in median, average, or variation of results. The results from the calculation without ground subsidence (Case C4) only exhibited a slight milder shoreline retreat compared to Cases C1-C3.

The results calculated under different volumes of sediment discharge to undersea valley (cases S1-S3) also did not show significant differences in shoreline change. However, this result is highly dependent on the location of the survey line, as survey line #36 (x = 6,260 m) is situated upstream of longshore drift than the undersea valley (x= 1,000-2,000 m). Shoreline changes variated near the undersea valley (Fig. 6.), indicating that the difference in sediment discharge to undersea valley has a local impact on the Suruga coast.

Differences in sea level resulted in slight variations in future shoreline changes. The median and average values of shoreline retreat decreased as the sea level declined from the 95% upper limt (Case W2) to the 95% lower limt (Case W4). However, these differences were smaller than the variation of results within each sea level condition (Cases W2, W3 and W4; Fig. 7). The variation of shoreline change within the same sea level deminished under the RCP8.5 scenario (cases W5-W7), and the differences among different sea level conditions became more pronounced than in the senario RCP2.6 (cases W2-W4).

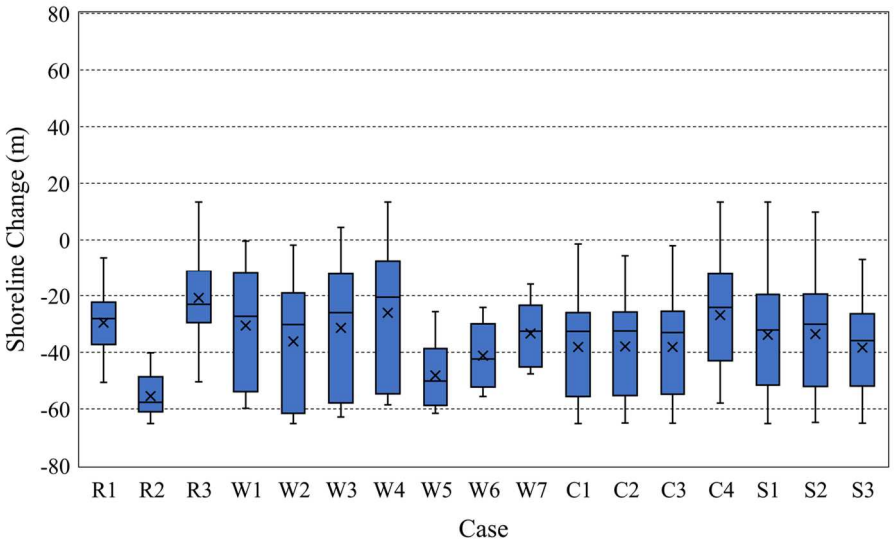

Figure 7. Variations in calculated shoreline changes among cases extracted under the same condition in survey line #36 (longshore distance x = 6,260 m). Symbols R1-R3, W1-W7, C1-C4, and S1-S3 represent the conditions used for extracting the cases. The box plots for R1-R3, W1-W7, C1-C4, and S1-S3 were derived from the calculation results of 84, 36, 63 and 84 cases, respectively.

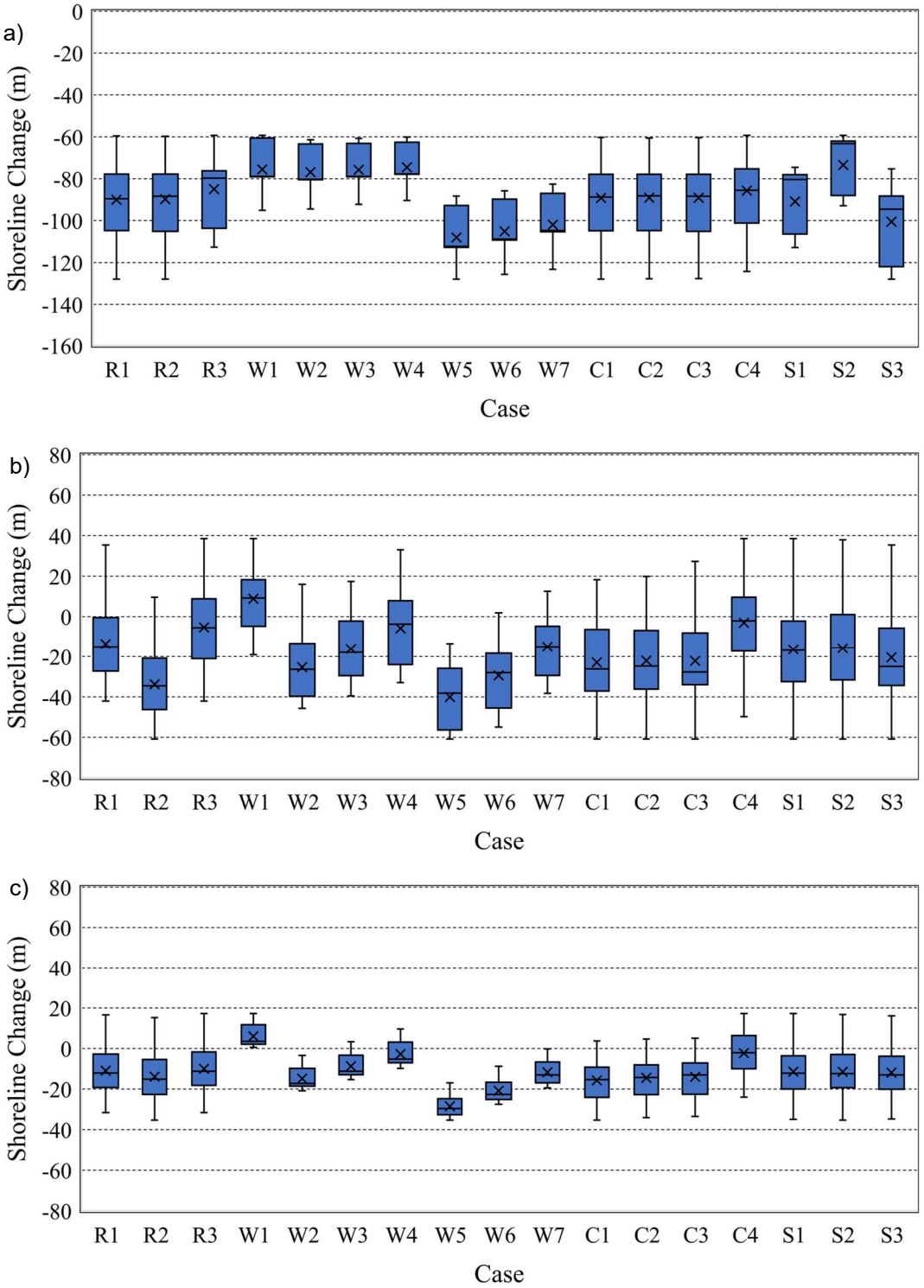

Figure 8. Variations in calculated shoreline changes among cases extracted under the same condition. a) survey line #5 (longshore distance x = 570 m), b) survey line #74 (x = 13,380 m), c) survey line #89 (x = 16,190 m).

These trends observed in survey line #36 were also confirmed in many other survey lines. However, different trends were observed in some survey lines, such as showed in Fig. 8. In survey line #5, located

near the northern end of the coast, differences in sediment supply from the river (cases R1-R3) did not affect the variation in calculation results (Fig. 8a). In contrast, differences in sediment discharge (cases S1-S3) resulted in variations in shoreline change (Fig. 8a). Conversely, focusing on the area south of the Oi River, sediment supply from the river significantly influenced the results in suvey line #74 (Fig. 8b), similar to survey line #36 (Fig. 7). However, in line 89, which is located further down drift from line 36, the influence of sediment supply was smaller, and differences in sea level and wave conditions (cases W1-W7) had a greater impact (Fig. 8c).

DISCUSSIONS

Consistency of the Simulation Model with the Bruun Rule

Our simulation model was validated by calculating the shoreline change on a model beach with 1 mm grain size and comparing it to the shoreline change calculated by using Bruun rule. The calculated beach profile closely matched the result of Bruun rule. This result suggests that our simulaiton model is applicable to beaches composed of sediment sizes below 1.09 mm, where parameters for the equilibrium profile are provided by Dean (2002). Given that this model is physics-based, it is considered applicable to coastal areas where the sediment size exceeds 1.09 mm. However, due to the lack of comparable and verifiable data, future data collection through experiments and field observations is necessary.

Serizawa et al. (2003) combined the stabilization mechanism of the beach profile with the contour-line change model developed by Uda and Kawano (1996). Serizawa et al. (2003) introduced the equilibrium slope of sand (β_c), where the shoreward motion of sand particles due to wave action is assumed to be balanced with the seaward motion due to gravity at this angle. This concept is based on the work of Bakker (1968). While the equilibrium profile used by Dean (2002) was statistically derived from field data, the angle β_c proposed by Serizawa et al. (2003) was developed based on physical principles. Despite this methodological difference, they are essentially equivalent. Therefore, the cross-sectional profiles obtained from the Bruun rule and those derived from shoreline change model are considered to be generally consistent.

Advantages of the Modified Contour Line Change Model

Our model calculates the future shoreline change based on physical principles, taking into account the gradual changes of various factors such as sea level, wave conditions, and sediment supplies. In contrast, the Bruun rule-based models (e.g. Dean and Houston 2016) can only estimate shoreline change at a single future time point. Since actual future changes occur gradually, our model is considered to provide more realistic predictions. These differences might be one of the cause of the slight difference observed in shoreline change on a model beach with simple topography (Fig. 5). Additionally, our model has the advantage of being able to calculate shoreline changes on coasts composed of mixed-size sediments.

However, when applying our model to other coasts, special attention should be given to the setting of the stable slope angle β_C (Eq. 2). In this study, we determined the angle β_C based on the relationship between grain sediment size and stable slope angle, compiled from coasts in Japan. As mentioned earlier, the stable slope angle is also influenced by wave conditions. Therefore, on coasts where the wave conditions differ significantly from those in Japan, the stable slope angle β_C must be carefully investigated.

Sources of Uncertainty

Hawkins and Sutton (2009) proposed three main sources of projection uncertainty: internal variability, model uncertainty, and scenario uncertainty. Internal variability refers to the natural fluctuations produced by the planet without any radiative focing, such as the pacific Decadal Oscillation (Wu et al. 2022). Model uncertainty arises from differences in implementations of numerical methods, varied mathematical expressions, and diverse parameterization processes. Scenario uncertainty is mainly induced by differences in assumptions about future population levels and pathways of economic and social development. The uncertainty we investigated falls under scenario uncertainty. Most of scenario uncertainty is associated with Representative Concentrarion Pathways (RCPs) emissions scenarios and Shared Socioeconomics Pathways (SSPs).

This study demonstrated that the most of future shoreline variations were mainly induced by differences in sediment supply from the river. The results suggest that the local factors, such as sediment supply, can be more important for projecting future changes on a local scale. This finding indicates that improving the accuracy of predictions for sediment supply from rivers is crucial for enhancing the

precision of future shoreline change projections. From the perspective of climate change adaptation, increasing sediment supply from rivers could help maintain shorelines even in the face of SLR. It is essential to advance comprehensive sediment management of the sedimentary system from mountains to the sea, which is beginning to take shape along various coasts in Japan (Kato et al. 2023).

However, there were also survey lines where the influence of other factors was stronger than that of sediment supply from rivers. The results for both survey lines #5 and #74, located far from the river mouth, suggest that local factors such as sediment discharge have a greater impact in areas distant from sediment sources (Fig. 8a and Fig. 8b). Caution is necessary in locations such as the ends of the coastline. However, these results may be due to the fact that the Suruga coast is an eroding coastline where sediment does not sufficiently reach both ends of the coast. On generally accreting beach, the influence of sediment supply may also be strong at the ends.

Ground Subsidence by Tectonics

In this study, the timing differences of crustal deformation did not significantly affect the calculation results (Fig.7 and Fig.8). However, it is important to note that this may be due to the limitations of the computational methods used in this research. In the contour change model, phenomena such as crustal deformation, where elevation changes discontinuously, may not be accurately represented in calculations. Therefore, we cannot definitively state that crustal deformation has minimal impact.

CONCLUSIONS AND FUTURE PERSPECTIVES

Future shoreline changes on the Suruga Coast were projected using a modified contour line change model that considers uncertain factors, including sea level, wave characteristics, ground subsidence, sediment supply from rivers, and sediment loss to undersea valley. The contributions of each factor to variations in shoreline changes were evaluated, revealing the importance of accurately estimating sediment supply from rivers. The evaluation scheme of this research is applicable to beaches where erosion due to rising sea levels is suspected, providing valuable insights for determining the significant factors for shoreline change projections.

This study set three conditions for each factors: the mean, upper bound, and lower bound. However, this approach has the shortage of resulting in a very wide range of uncertaity. While it is important to consider the worst-case scenario, excessive conditional settings can pose constraints on planning climate change adaptation. Each factors should be provided with probability distributions to make the projected results more practical. This should be addressed in future research.

ACKNOWLEDGMENTS

The authors would like to thank Professor Tomoya Shimura in Disaster Prevention Research Institute, Kyoto University, for providing us with the result of future wave climate projections. The authors acknowledge that Professor Nobuhito Mori in Disaster Prevention Research Institute, Kyoto University, and Professor Tomoya Shimura gave us valuable suggestions throughout the course of this study, and that the Shizuoka Office of River (Ministry of Land, Infrastructure, Transport and Tourism Chubu Regional Development Bureau) provided us with survey data and historical records of coastal conservation efforts in Suruga Coast (e.g. construction of breakwaters, beach nourishment).

REFERENCES

Bakker, W. T. 1968. The dynamics of a coast with groyne system, *Proc. 11th Int. Conf. on Coastal Engineering*, 492-517. https://doi.org/10.1061/9780872620131.031

Başaran, B., and H. A. Arı Güner. 2024. Future wave climate-driven longshore sediment transport and shoreline evolution along the southern Black Sea, *Water*, 16, 1787. https://doi.org/10.3390/w16131787

Bruun, P. 1983. Review of conditions for use of the Bruun rule of erosion, *Coastal Engineering*, 7, 77-89. https://doi.org/10.1016/0378-3839(83)90028-5

Cooper, J. A. G., and O. H. Pilkey. 2004. Sea-level rise and shoreline retreat: time to abandon the Bruun rule, *Global and Planetary Change*, 43, 157-171. https://doi.org/10.1016/j.gloplacha.2004.07.001

Dean, R. G. 2002. *Beach Nourishment: Theory and Practice*, *World Scientific*, 399 pp.

Dean, R.G., and J. R. Houston. 2016. Determining shoreline response to sea level rise, *Coastal Engineering*, 114, 1-8. https://doi.org/10.1016/j.coastaleng.2016.03.009

Hawkins, E., and R. Sutton. 2009. The potential to narrow uncertainty in regional climate predictions. Bulletin of the American Meteorological Society, 90(8), 1095–1108. https://doi.org/10.1175/2009BAMS2607.1

Isobe, M., Y. Xiping, K. Umemura, and S. Takahashi. 1999. Study on development of numerical wave flume, *Proceedings of Coastal Engineering, JSCE*, 46, 36-40. (in Japanese) https://doi.org/10.2208/proce1989.46.36

Kato, F., and Y. Tajima. 2023. Coastal adaptation to climate change in Japan: a review. *Coastal Engineering Journal*, 65(4), 597–619. https://doi.org/10.1080/21664250.2023.2259187

Kumada, T., A. Kobayashi, T. Uda, M. Serizawa, Y. Hoshigami, and K. Masuda. 2002. Development of a model for predicting beach changes considering sorting of sand of mixed grain size, *Proceedings of Coastal Engineering, JSCE*, 49, 476-480. (in Japanese) https://doi.org/10.2208/proce1989.49.476

Kumada, T., T. Uda, M. Serizawa, and Y. Noshi. 2007. Model for predicting changes in grain size distribution of bed materials, *Coastal Engineering 2006*, 3043-3055. http://dx.doi.org/10.1142/9789812709554_0256

MEXT, and JMA (Ministry of Education, Culture, Sports, Science and Technology, and Japan Meteorological Agency). 2020. *Climate Change in Japan 2020 -Report on Assessment of Observed/Projected Climate Change Relating to the Atmosphere, Land and Oceans*, 15 pp. https://www.data.jma.go.jp/cpdinfo/ccj/2020/pdf/cc2020_gaiyo_en.pdf.

Ozasa, H., and A. H. Brampton. 1980. Mathematical modelling of beaches backed by seawalls, *Coastal Engineering*, 4, 47-63. https://doi.org/10.1016/0378-3839(80)90005-8

Ranasinghe, R. 2012. Estimating coastal recession due to sea level rise: beyond the Bruun rule, *Climate Change*, 110, 561-574. https://doi.org/10.1007/s10584-011-0107-8

Ranasinghe, R. 2016. Assessing climate impacts on open sandy coasts: A review, *Earth-Science Reviews*, 160, 320-332. https://doi.org/10.1016/j.earscirev.2016.07.011

Serizawa, M., T. Uda, T. San-nami, K. Furuike, and T. Kumada. 2003. Improvement of contour line change model in terms of stabilization mechanism of longitudinal profile, *Coastal Sediments '03*, 1-15.

Shimura, T., and N. Mori. 2019. Future projection of spectral wave climate around Japan, *Journal of Japan Society of Civil Engineers*, *Ser. B2(Coastal Engineering)*, 75(2), I_1177-I_1182. (in Japanese) http://dx.doi.org/10.2208/kaigan.75.I_1177

Tanaka, H., and M. Suzuki. 1998. Predictive model of shoreline change and grain-size sorting, *Proceedings of Coastal Engineering, JSCE*, 45, 511-515. (in Japanese) https://doi.org/10.2208/proce1989.45.511

Toimil, A., P. Camus, I. J. Losada, G. Le Cozannet, R. J. Nicholls, D. Idier, and A. Maspataud. 2020. Climate change-driven coastal erosion modelling in temperate sandy beaches: Methods and uncertainty treatment, *Earth-Science Reviews*, 202, 103110. https://doi.org/10.1016/j.earscirev.2020.103110

Uda, T., and S. Kawano. 1996. Development of a predictive model of contourline change due to waves, *Doboku Gakkai Ronbunshu*, 539, 121-139. (in Japanese) https://doi.org/10.2208/jscej.1996.539_121

Udo, K., and Y. Takeda. 2017. Projections of future beach loss in Japan due to sea-level rise and uncertainties in projected beach loss, *Coastal Engineering Journal*, 59:2, 1740006-1-1740006-16. https://doi.org/10.1142/S057856341740006X

Watanabe, K., F. Kato, Y. Tanaka, and A. Katano. 2024. Bias correction on spectral wave climate for projecting beach change under future climate scenarios. Japanese Journal of JSCE, 80(17), 24-17265. (in Japanese) https://doi.org/10.2208/jscejj.24-17265

Wu, Y., C. Miao, X. Fan, J. Gou, Q. Zhang, and H. Zheng. 2022. Quantifying the uncertainty sources of future climate projections and narrowing uncertainties with bias correction techniques, Earth's Future, 10, e2022EF00296. https:doi.org/10.1029/2022EF002963